BJ www.biochemj.org

BJ Disease

Biochem. J. (2008) **413**, 305–313 (Printed in Great Britain) doi:10.1042/BJ20071357

online data

Membrane pore formation by pentraxin proteins from *Limulus*, the American horseshoe crab

John M. HARRINGTON*†[1], Hui-Ting CHOU*, Thomas GUTSMANN‡, Christoph GELHAUS§, Henning STAHLBERG*, Matthias LEIPPE†§ and Peter B. ARMSTRONG*†

*Department of Molecular and Cellular Biology, University of California, One Shields Avenue, Davis, CA 95616, U.S.A., †Marine Biological Laboratory, Woods Hole, MA 02543, U.S.A., ‡Division of Biophysics, Research Center Borstel, Parkallee 10, D-23845 Borstel, Germany, and §Zoological Institute of the University of Kiel, Olshausenstr. 40, D-24098 Kiel, Germany

The pentraxins are a family of highly conserved plasma proteins of metazoans known to function in immune defence. The canonical members, C-reactive protein and serum amyloid P component, have been identified in arthropods and humans. Mammalian pentraxins are known to bind lipid bilayers, and a pentraxin representative from the American horseshoe crab, *Limulus polyphemus*, binds and permeabilizes mammalian erythrocytes. Both activities are Ca^{2+}-dependent. Utilizing model liposomes and planar lipid bilayers, in the present study we have investigated the membrane-active properties of the three pentraxin representatives from *Limulus* and show that all of the *Limulus* pentraxins permeabilize lipid bilayers. Mechanistically, *Limulus* C-reactive protein forms transmembrane pores in asymmetric planar lipid bilayers that mimic the outer membrane of Gram-negative bacteria and exhibits a Ca^{2+}-independent form of membrane binding that may be sufficient for pore formation.

Key words: C-reactive protein, innate immunity, invertebrate, liposome, pentraxin, pore formation.

INTRODUCTION

Pentraxin proteins are characterized by a highly conserved secondary structure and cyclic oligomeric symmetry [1]. Representative pentraxins have been identified in the plasma of diverse metazoan lineages including humans and arthropods, where they contribute to immune defence. The canonical member, CRP (C-reactive protein) was first isolated from the sera of acute phase patients by, and subsequently named for, its ability to precipitate C-polysaccharide from *Streptococcus pneumoniae* [2,3]. Clinically, CRP levels are used as important markers for determining the risk and/or the severity of an assortment of diseases including bacterial sepsis, atherosclerosis, autoimmune diseases and some forms of cancer [4,5]. Mammalian pentraxins include serum amyloid P component [6], a ubiquitous component of amyloid plaques, and the relatively newly identified long pentraxins, that include PTX3, a secreted pattern-recognition receptor important for innate immune defence against fungal pathogens [7,8]. Multiple pentraxin proteins have also been identified in horseshoe crabs, long-lived marine invertebrates. These organisms provide a model system to study the role of the pentraxins in immune protection where these proteins are particularly relevant due to the lack of adaptive immunity in the invertebrate lineages.

The pentraxin orthologues from *Limulus* consist of L-CRP (*Limulus*-CRP) [9–11] and L-SAP (*Limulus* serum amyloid P component) [12,13], both of which are also present in mammals, and limulin, which is the sole haemolytic protein from the plasma of *Limulus* [9,14–16]. This suite of pentraxins is present at a concentration of 1–7 mg/ml (2.9–20 μM) in the plasma of *Limulus*, and represents the second most abundant class of proteins in the haemolymph, behind haemocyanin [17]. The individual pentraxins are functionally characterized by differing affinities for phosphoamino compounds and glycoconjugates, with L-CRP and limulin binding both phosphorylcholine and phosphorylethanolamine, L-SAP binding only phosphorylethanolamine, and limulin uniquely able to bind sialic acid [12,14–16]. These Ca^{2+}-dependent activities allow for a simple affinity-chromatography method for separating the individual LPx (*Limulus* pentraxins) from one another [12,16]. Structurally, the LPx exist as cyclic oligomers of doubly stacked rings of 6–8 monomers [9,12,18]. Electron microscopy reveals a large central pore of 2.0–4.0 nm [19].

It has been shown that limulin permeabilizes mammalian erythrocytes in a Ca^{2+}-dependent fashion [16]. Permeabilization of membranes is a well-known tactic in immune defence exhibited by a variety of antimicrobial peptides and the vertebrate complement system [20–22]. Mechanistically, limulin-induced haemolysis results from osmotic swelling caused by the insertion of the protein across the cell membrane to form hydrophilic pores of a diameter too small to allow efflux of cytoplasmic proteins but large enough to admit water molecules. This hypothesis is supported by the ability of the macromolecular osmolites dextran-4 and -8 in the bathing medium to reversibly protect erythrocytes from limulin-mediated haemolysis. The extracellular polydextrans are imagined to equalize the osmotic pressure of the cytoplasmic proteins, predominantly haemoglobin, inside the limulin-permeabilized erythrocyte by virtue of their inability to pass across the membrane via the transmembrane pores of limulin and thereby protecting the cell from osmotic swelling and cytolysis. An estimate for a functional pore size of 1.7 nm has been derived from the size of the smallest dextran capable of protecting from haemolysis [23].

Limulin targets mammalian erythrocytes by binding sialic acid residues on the surface of the cell [16,18]. The lack of haemolytic activity from L-CRP and L-SAP may be due to their

Abbreviations used: CrCRP, *Carcinoscorpius rotundicauda* C-reactive protein; CRP, C-reactive protein; L-CRP, *Limulus*-CRP; LPS, lipopolysaccharide; LPx, *Limulus* pentraxins; L-SAP, *Limulus* serum amyloid P component; PC, phosphatidylcholine; PE, phosphatidylethanolamine; PI, phosphatidylinositol; PS, phosphatidylserine; RP, reversed-phase; TEM, transmission electron microscope; TFA, trifluoroacetic acid.

[1] To whom correspondence should be addressed at the present address: Department of Biochemistry and Molecular Biology, Life Sciences Building, University of Georgia, Athens, GA 30602, U.S.A. (email jmharrin@uga.edu).

failure to bind at the surface of the erythrocyte. It has long been known that mammalian CRP binds lipid bilayers containing accessible phosphorylcholine moieties [24,25], e.g. oxidized phosphatidylcholine. Presumably, this provides a mechanism for distinguishing between healthy cells, which CRP does not bind, and damaged cells, for which CRP participates in their removal. Previously, it has been shown that CRP from the Southeast Asian species of horseshoe crab, *Carcinoscorpius rotundicauda*, (termed CrCRP) is an LPS (lipopolysaccharide)-binding protein [26]. LPS is the major lipid component of the outer membrane of Gram-negative bacteria. Additionally Ng et al. [27] have identified a complex of plasma proteins, namely galactose-binding protein and carcinolectin-5, which facilitates the deposition of CRP on bacterial membranes that were previously not thought to be CRP targets [27]. These results suggest that horseshoe crab pentraxins perform a critical function at the membrane of potential pathogens. The antimicrobial properties of the LPx are incompletely characterized: pentraxins from Asian species of horseshoe crabs have been reported to bind [27], agglutinate and inhibit the growth of Gram-negative bacteria [28]. In an effort to characterize the membrane-active properties of the pentraxins from *Limulus*, we investigated the interaction of these proteins with artificial cell membranes using a simplified system of model liposomes and planar lipid bilayers.

EXPERIMENTAL

Lipids

Soy bean azolectin was purchased from both Sigma and Avanti Polar Lipids. Monogalactosyldiacylglycerol and digalactosyldiacylglycerol were purchased from Lipid Products. Total and polar extracts of *Escherichia coli* lipids, polar extracts of soy lipids, PC (phosphatidylcholine), PE (phosphatidylethanolamine), PI (phosphatidylinositol), PS (phosphatidylserine), sphingomyelin, cardiolipin and cholesterol were purchased from Avanti Polar Lipids.

For the preparation of reconstituted membranes, deep rough mutant LPS from *E. coli* strain WBB01 was used. LPS was extracted by the phenol/chloroform/petroleum ether method [29], purified, freeze-dried and transformed into the triethylamine salt form. PE from *E. coli*, phosphatidylglycerol from egg yolk lecithin and synthetic cardiolipin were purchased from Avanti Polar Lipids and used without further purification.

Protein purification

Adult *Limulus* were purchased from the Marine Resource Center at the Marine Biological Laboratory in Woods Hole, MA, U.S.A. Methods for collection, processing and treatment and storage of *Limulus* haemolymph have been described previously [13,16,23,30]. Animals were initially chilled (4 °C, 2–4 h) to retard exocytosis of the blood cells, and then bled under sterile conditions by direct cardiac puncture. After bleeding, the animals were released into the ocean unharmed. Haemocytes were immediately removed by centrifugation (2000 ***g*** for 10 min at 25 °C) and the resulting plasma was stored at 4 °C with 0.02 % sodium azide. The LPx were purified from plasma by a three-step affinity-chromatography procedure [16]. Plasma was initially depleted of haemocyanin, by incubation with 3 % poly(ethylene glycol)-8000 and centrifugation at 30000 ***g*** for 30 min. Sepharose-binding proteins were eliminated by passage of haemocyanin-depleted plasma over Sepharose 4B. This fraction was then applied to phosphorylethanolamine–agarose equilibrated with buffer A [0.15 M NaCl, 10 mM $CaCl_2$, 50 mM Tris/HCl (pH 7.4)]. The resin was washed with buffer A containing 1 M NaCl and the LPx were eluted with 0.1 M sodium citrate. This sample was re-calcified and fractionated into the individual pentraxins. Limulin was separated from the LPx mixture by passage of this material over fetuin–Sepharose. The break-through fraction contains L-CRP and L-SAP. Multiple passages over fetuin–Sepharose were employed to remove all traces of limulin, which was then subsequently eluted with 0.1 M sodium citrate. The remaining pentraxins were reapplied to phosphorylethanolamine–agarose and the column was washed, exhaustively, with 100 mM PC in buffer A. This step elutes L-CRP. L-SAP, which lacks PC-binding capability, remains bound and is subsequently eluted with 10 mM EDTA [12]. The individual LPx were dialysed with buffer A plus 1 mM citrate and stored at 4 °C in the presence of 0.02 % sodium azide. Preparation of the LPx by this procedure results in apparent homogeneity of each individual LPx as evidenced by silver-stained SDS/PAGE gels.

A portion of the L-CRP fraction was subjected to RP (reversed-phase) HPLC using a PRP-3 column (Hamilton) connected to a 130A separation system (Applied Biosystems) and equilibrated with 0.1 % TFA (trifluoroacetic acid). The column was washed with 0.1 % TFA (3 min) and proteins were eluted with a linear gradient of 0–84 % acetonitrile, 0.1 % TFA for 45 min and at a flow rate of 0.2 ml/min. L-CRP was eluted with 46 % acetonitrile from the column (Supplementary Figure S1 at http://www.BiochemJ.org/bj/413/bj4130305add.htm). N-terminal sequencing of the first 20 residues of L-CRP purified by RP-HPLC was accomplished with a gas-phase protein sequencer (model 437 A; Applied Biosystems) and revealed a single sequence corresponding to L-CRP 1.1 [10] (LEEGEITSKVKFPPSSSPSF). The identity of the purified L-CRP 1.1 was confirmed by MS/MS (tandem MS) using a MALDI–TOF (matrix-assisted laser-desorption ionization–time-of-flight) mass spectrometer (4700 Proteomics Analyser; Applied Biosystems) (results not shown).

Liposome diffusion potential assays

Diffusion potential-based assays were performed essentially according to Loew et al. [31]. Liposomes were prepared by hydration of a thin film of soy bean azolectin with liposome buffer [50 mM K_2SO_4 and 50 mM Tris/maleate (pH 5.2)]. The resulting liposomes (40 mg of lipid/ml, final concentration) were subject to sonication and freeze-thawing according to Pick [32]. Assays were conducted by diluting liposomes 1:4000 in cuvette buffer (liposome buffer but with Na^+ substituted for K^+). Unless otherwise noted, all assays were performed in cuvette buffer (pH 5.2). Addition of the K^+ ionophore valinomycin to a final concentration of 1 nM induced a diffusion potential that was monitored by the fluorescent self-quenching of the cationic, lipophilic dye 3,3′-diethylthiodicarbocyanine iodide [diS-C_2-(5), 1 μM]. Soy bean azolectin was employed in these assays because it was the only lipid composition that facilitated immediate dye quenching upon the addition of valinomycin. Permeabilization of liposomes was seen as fluorescent intensity recovery with pre-valinomycin fluorescent intensity used as the 100 % permeabilization value. A unit of activity is arbitrarily defined as an initial fluorescent intensity increase of 5 % per min of the 100 % fluorescence value. Fluorescence was monitored with a luminescence spectrophotometer (PerkinElmer, LS50B) with excitation and emission values of 620 nm and 670 nm respectively, both with 10 nm slit widths.

Calcein release

Lipid films were hydrated in the presence of 30 mM calcein (Molecular Probes), with 10 mM Hepes to a lipid concentration of 10 mg/ml. The resulting multilamellar liposomes were made unilamellar by extrusion through a 0.1 μm polycarbonate filter (15 passages). Untrapped calcein was removed from solution by gel filtration using Sephacryl S-300 HR. Permeabilization of these liposomes was indicated by a fluorescent intensity increase (excitation 484 nm, emission 513 nm, 2.5 nm slit widths). Fluorescent intensities corresponding to 100 % lysis were acquired from calcein leakage assays by the addition of Triton-X 100 to a final concentration of 0.01 %. A unit of activity is arbitrarily defined as an initial fluorescent intensity increase of 5 % per min of the 100 % fluorescence value.

Kinetic analysis of calcein leakage

Traces were acquired using a single liposome preparation of total *E. coli* lipids and a constant concentration of 10 mM $CaCl_2$. A single preparation of L-CRP was serially diluted in its identical storage buffer (buffer A) for addition to each assay. The time-resolved traces were sampled at 30 s intervals after the addition of L-CRP and values for percentage retained dye (R) were calculated as:

$$R = [(I_f - I_0) - (I_t - I_0)]/(I_f - I_0) \times 100$$

where I_f is the emission intensity at 100 % dye efflux, i.e. after the addition of Triton, I_0 is the emission intensity before any dye efflux, i.e. background signal, and I_t is the measured fluorescence intensity at any given time. The natural log of the percentage retained dye was plotted against time.

Preparation of planar bilayers and electrical measurements

Planar bilayers were prepared according to the Montal–Mueller technique [33] as described previously [34]. Briefly, asymmetric bilayers were formed by opposing two lipid monolayers prepared on aqueous subphases from chloroformic solutions of the lipids at a small aperture ($\varnothing \sim 150\ \mu$m) in a thin Teflon septum. The inner leaflet of the outer membrane of Gram-negative bacteria was reconstituted by a phospholipid mixture consisting of PE, phosphatidylglycerol and cardiolipin (molar ratio 81:17:2) [35,36]. The outer leaflet was composed of LPS extracted from *E. coli* WBB01. For electrical measurements, planar membranes were voltage-clamped via a pair of Ag/AgCl-electrodes (type IVM E255, Advanced Laboratory Research) connected to the head-stage of an L/M-PCA patch-clamp amplifier (List-Medical). In all experiments, the compartment to which L-CRP was added is named first (*cis*), and the compartment opposite to the addition (*trans*) was grounded. Therefore in comparison with the natural system, a positive clamp-voltage represents a membrane that is negative on the inside. All measurements were performed at a temperature of 37 °C with bathing solutions consisting of 100 mM NaCl and 10 mM $CaCl_2$ buffered with 5 mM Hepes and adjusted to pH 5.2. At the beginning of each experiment, membrane formation was checked by measuring membrane current and capacitance. Only membranes with a basic current of less than ± 2.5 pA at clamp-voltages of ± 100 mV and a capacitance > 100 pF were used for the experiments.

90° light scattering

Liposomes were constructed from total *E. coli* lipids and made unilamellar by extrusion through a 0.1 μm polycarbonate membrane. Assay conditions were the same as those described for the diffusion potential assays. The 90° light-scattering intensity was monitored over time with the PerkinElmer LS50B. Excitation and emission wavelengths were both set to 405 nm with 10 nm slit widths.

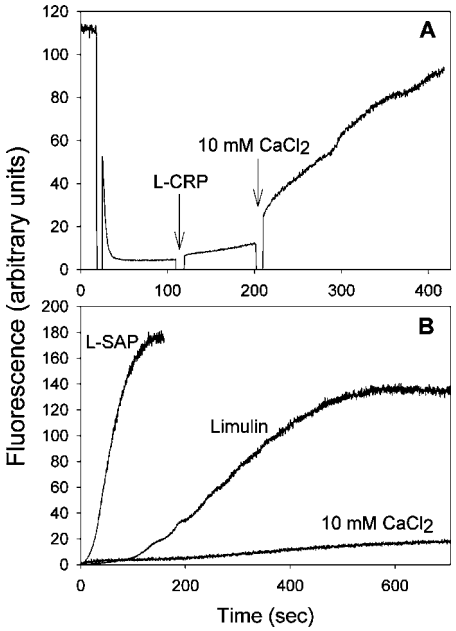

Figure 1 Liposome permeabilization by the LPx

A valinomycin-induced K^+-diffusion potential was established in unilamellar azolectin liposomes and monitored in cuvette buffer, pH 5.2, with the cationic self-quenching fluorescent dye diS-C_2-(5). (**A**) Addition of 5 nM HPLC-purified L-CRP alone has no significant effect on the diffusion potential maintained by liposomes. Subsequent addition of 10 mM $CaCl_2$ facilitates permeabilization by L-CRP. (**B**) Affinity-purified L-SAP and limulin exhibit similar liposome-permeabilizing activity. Traces were obtained in the presence of 10 mM $CaCl_2$ and do not illustrate the initial setup of the diffusion potential, i.e. the addition of protein is zero time. Addition of $CaCl_2$ in the absence of protein has no effect.

Electron microscopy

Unilamellar liposomes constructed from total *E. coli* lipids (100 μg/ml), and prepared by extrusion, were incubated with 0.2 μM L-CRP in 50 mM Tris/maleate and 50 mM Na_2SO_4 (pH 5.2) with or without 10 mM $CaCl_2$ for approx. 30 s and 25 min respectively. Lipid and protein samples were adsorbed to glow-discharged, carbon-coated copper grids and stained with 2 % uranyl acetate. Samples were imaged with a JEOL JEM-1230 TEM (transmission electron microscope).

RESULTS

Limulus pentraxins permeabilize lipid bilayers

In order to investigate the lipid bilayer permeabilizing activity of the LPx we monitored their effects on the integrity of model liposomes with two fluorescence-based assays. Addition of L-CRP to liposome suspensions, (i) rendered unilamellar vesicles incapable of retaining entrapped calcein, and (ii) resulted in the dissipation of a valinomycin-induced K^+-diffusion potential. Permeabilizing activity was divalent-cation-dependent (Figure 1A). We found robust activity at nanomolar L-CRP concentrations (e.g. 25 nM), approx. an order of magnitude lower than the concentration of the protein in the haemolymph [17]. The

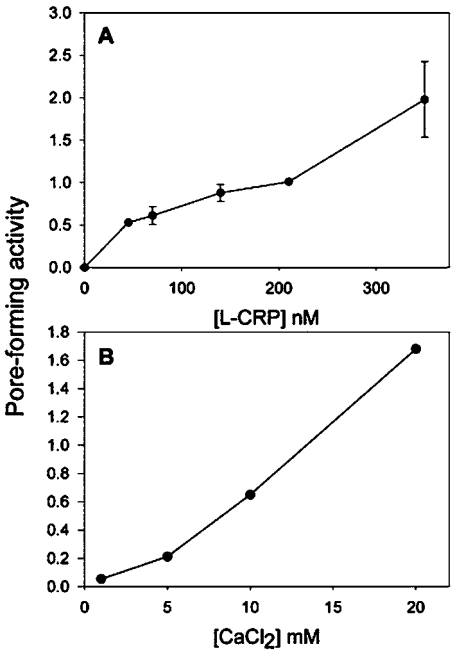

Figure 2 Dose- and Ca^{2+}-dependence of L-CRP-mediated liposome permeabilization

The collapse of a valinomycin induced K^+-diffusion potential (in unilamellar azolectin liposomes) was monitored in cuvette buffer, pH 5.2, (**A**) with 10 mM $CaCl_2$ and various concentrations of L-CRP or (**B**) at a constant L-CRP concentration of 25 nM with increasing concentrations of $CaCl_2$. Data points are the average of at least duplicates and, where applicable, error bars represent the S.D.

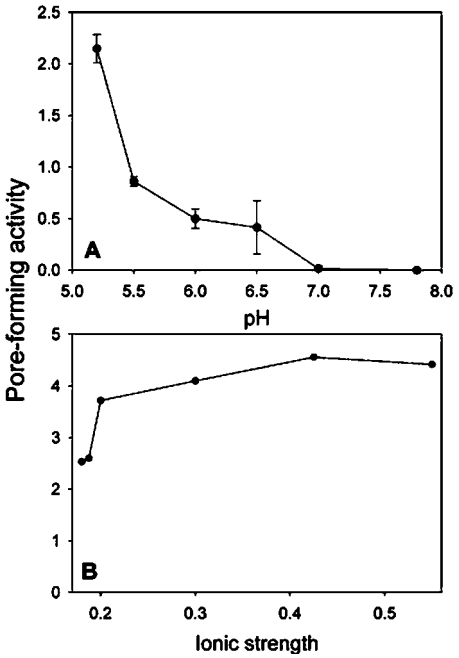

Figure 3 pH- and ionic-strength-dependence of L-CRP-mediated liposome permeabilization

(**A**) Liposomes constructed from total lipid extracts of *E. coli* were assayed for calcein leakage in the presence of 25 nM L-CRP and 10 mM $CaCl_2$ at varying pH. (**B**) Identical liposomes were assayed for calcein leakage in cuvette buffer, pH 5.2, with 25 nM L-CRP, 10 mM $CaCl_2$ and increasing concentrations of NaCl. Data points are the average of at least duplicates and, where applicable, error bars represent the S.D.

other pentraxins, limulin and L-SAP, also exhibit significant permeabilizing activity against liposomes composed of soy azolectin (Figure 1B). Different batches of azolectin yielded variable levels of activity for these LPx. Liposome-permeabilizing activity of L-CRP increased in a dose-dependent manner and was directly proportional to Ca^{2+} concentrations up to 10 mM, the concentration of Ca^{2+} found in plasma (Figure 2). Equimolar concentrations of $MgCl_2$ facilitated permeabilization by L-CRP to approx. 35 % of the activity afforded by $CaCl_2$ (results not shown). The ability of L-CRP to permeabilize liposomes was highest at pH 5.2, the lowest pH tested, and was unobservable at pH 7.8 (Figure 3A). Limulin and L-SAP exhibited similar dependence on low pH for permeabilizing activity (results not shown). L-CRP-elicited calcein leakage was robust at high ionic strength (Figure 3B). We did not observe calcein leakage in any assays lacking divalent cations, i.e. L-CRP did not elicit leakage in cuvette buffer pH 5.2, 750 mM NaCl.

Liposomes composed of mixed lipids of natural origin (e.g. total lipid extracts from *E. coli* and soy bean azolectin) were sensitive to permeabilization by L-CRP. Liposomes composed of the polar extracts of each lipid preparation were also permeabilized, but to a lesser extent (Figure 4). Liposomes constructed from purified egg PC or mixtures of egg PC/PE, PC/PI, PC/PS, PC/sphingomyelin, PC/cardiolipin, PC/cholesterol, PC/monogalactosyldiacylglycerol or PC/digalactosyldiacylglycerol (all 3:1 by mass) were insensitive to permeabilization. We found no permeabilizing activity against PC liposomes containing lyso-PE or lyso-PC.

In order to distinguish between pore formation and a large-scale disruption of lipid bilayer structure such as micellization, we employed a variation of the K^+-diffusion potential-based assay where L-CRP was added to the liposomes prior to the induction

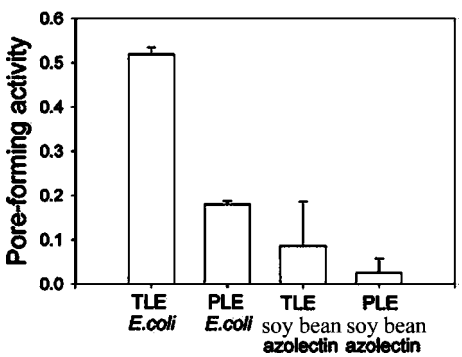

Figure 4 Susceptible liposomes are constructed from natural lipid preparations

Liposomes constructed from either the total (TLE) or polar (PLE) lipid extracts of *E. coli* or soy bean were assayed (in cuvette buffer, pH 5.2) for calcein leakage in the presence of 25 nM L-CRP and 10 mM $CaCl_2$. Values are means ± S.D. of triplicates.

of the diffusion potential, i.e. prior to the addition of valinomycin. These liposomes were capable of supporting a full, albeit transient, quenching of diS-C_2-(5) after valinomycin was added (Figure 5). Dye quenching is dependent on the presence of intact bilayers as the particular dye used in these assays intercalates into the outer leaflet of the bilayer by means of two short acyl chains, thus aggregating and ultimately self-quenching. After valinomycin effectively drives intercalation and self-quenching of the reporter dye, fluorescence recovery is quickly accomplished, indicating ionic equilibration across lipid bilayers. It is important to point out that once a K^+-diffusion potential is formed by the

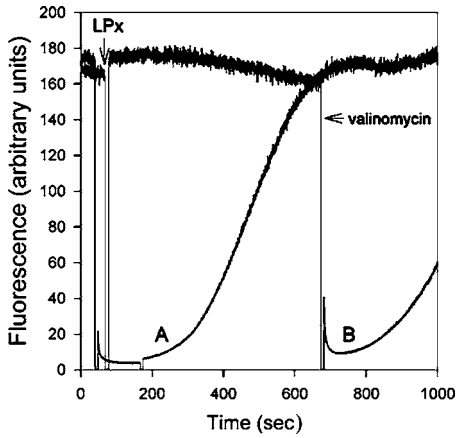

Figure 5 Pre-addition of LPx leaves the liposomes capable of supporting a full diffusion potential

Incubation of unilamellar azolectin liposomes with 40 nM mixed LPx in the presence of 10 mM $CaCl_2$ over a time period that allows for 100 % recovery of fluorescence prior to the addition of valinomycin leaves the liposomes capable of supporting a full quench of diS-C2-(5). (**A**) Trace obtained under 'normal' assay procedures where valinomycin is added prior to LPx. (**B**) Trace obtained with the pre-addition of LPx. Arrows indicate the addition of LPx or valinomycin.

action of valinomycin, the rate of Na^+ influx is greatly accelerated. Thus the rate of fluorescence recovery observed in the presence of both L-CRP and valinomycin is not indicative of the rate of cationic equilibration across the hydrophilic channels formed by L-CRP alone, but of a voltage-driven equilibration of Na^+ and K^+ ions. For a detailed discussion of this interpretation see Loew et al. [31].

Kinetics of L-CRP-induced calcein leakage

A plot of the natural log of percentage dye retained against time revealed two distinct phases in the progression of L-CRP-induced liposome permeabilization. A linear decline in percentage dye retained was preceded by an initial lag phase, during which no observable dye leakage occurred (Figure 6A). Restricting our analysis to the second phase, i.e. the linear decline in percentage retained calcein, we calculated first-order rate constants for the permeablization of liposomes composed of total *E. coli* lipids in cuvette buffer containing 10 mM $CaCl_2$ for 4.8, 9.3, 18.6 and 37.1 nM L-CRP (Figure 6B). A plot of the apparent rate constants against L-CRP concentration yielded a second-order rate constant of 2.66 nM^{-1} (Figure 6B, inset).

L-CRP forms pores in planar lipid bilayers

In order to define better the mechanism of pentraxin-mediated membrane permeabilization and establish a biological context, we performed electrical measurements on asymmetric planar lipid bilayers that mimic the outer membrane of Gram-negative bacteria. This was accomplished by constructing one leaflet of the bilayer from LPS that was extracted from *E. coli* WBB01 (outer leaflet) and the other leaflet from a mixture of phospholipids (inner leaflet). Addition of L-CRP to the side of the bilayer composed of LPS led to a decrease of the membrane capacitance (results not shown), a clear indication of membrane binding. Membrane binding was accompanied by an increase in electrical conductance across the bilayer (Figure 7), indicating that L-CRP molecules intercalate into the bilayer to form hydrophilic pores capable of facilitating movement of ions across the bilayer.

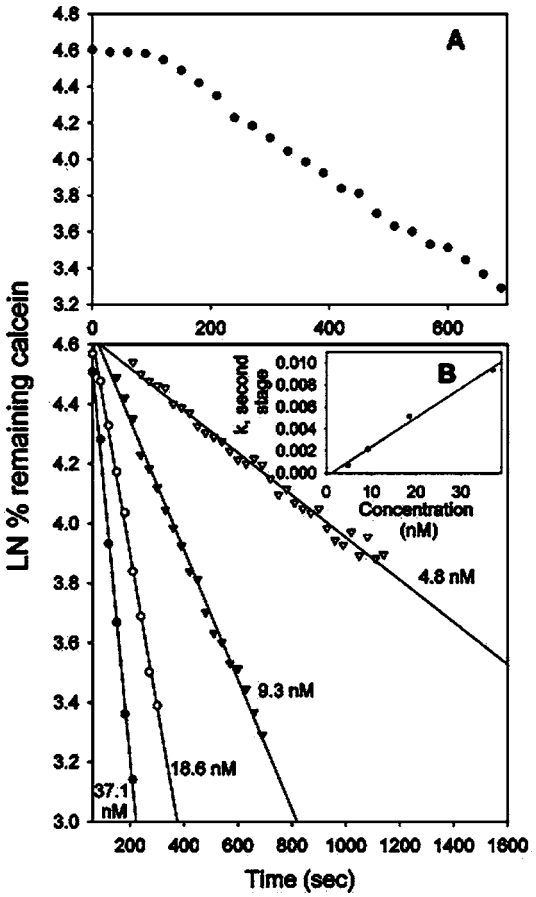

Figure 6 Kinetic analysis of L-CRP-mediated liposome permeabilization

Traces of L-CRP-induced leakage of calcein from liposomes composed of total *E. coli* lipids were analysed for rate constants. (**A**) Time-resolved plot of the natural log (LN) of the percentage of calcein remaining inside liposomes when treated with 9.3 nM L-CRP. The plot shows an initial lag phase followed by calcein leakage. (**B**) The linear portions of the plots of the natural log of the percentage of calcein remaining against time are fitted with a linear regression function. The inverse of the slope of each line reveals the first-order rate constant for L-CRP-induced calcein leakage. The slope of the line fit to the plot of first-order rate constants against L-CRP concentration gives the second-order rate constant for L-CRP-mediated permeabilization of liposomes constructed of *E. coli* lipids. This has a value of 2.66 nM^{-1}.

The pores induced by L-CRP are relatively stable; however, a flickering of the open-state could be observed. The opening and closing of the pores as well as the conductance of a single pore is voltage-dependent. At positive clamp-voltages (in correspondence to the inside negative voltage of the outer membrane of Gram-negative bacteria) the pores have a higher single-pore conductance and a higher probability to insert into the membrane or to be in the open-state. In contrast, at negative clamp-voltages, the pores tend to close. The mean diameter of a single membrane pore was estimated to be 1.9 ± 0.2 nm (see Supplementary material at http://www.BiochemJ.org/bj/413/bj4130305add.htm for the method of calculation).

L-CRP binds membranes in two different fashions

Limulin, L-SAP and L-CRP, as well as the pentraxins from *Tachypleus* [18], agglutinate *E. coli* (results not shown). Thus we asked whether L-CRP, in addition to permeabilizing target liposomes, also agglutinated them. Using 90° light scattering to monitor particle size we have found that L-CRP does indeed

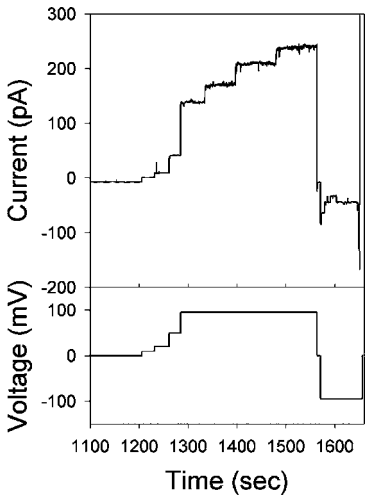

Figure 7 L-CRP forms pores in asymmetric LPS/phospholipid planar bilayers

Current fluctuations in asymmetric LPS/phospholipid bilayers are induced after the addition of 1 nM HPLC-purified L-CRP. The current is shown in the upper trace and the applied clamp voltage across the bilayer in the lower trace (*trans* side grounded). Bathing solution: 100 mM NaCl, 10 mM $CaCl_2$, 5 mM Hepes (pH 5.2), at 37 °C. The opening of single pores is revealed by the stepwise increase in current at positive clamp voltages. The membrane broke at time point t = 1650 s.

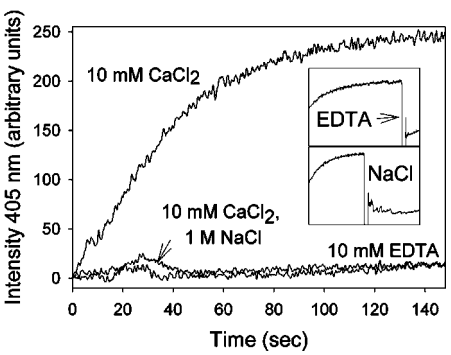

Figure 8 Liposomes are agglutinated by L-CRP

The 90° light-scattering intensity (405 nm) of a suspension of unilamellar liposomes constructed from total *E. coli* lipids was monitored as an indicator of relative particle size. A rapid increase in 90° light-scattering intensity is seen upon the addition of 25 nM L-CRP in cuvette buffer, pH 5.2, and the presence of 10 mM $CaCl_2$. The signal is sensitive to, and indeed fully reversed by (inset), the addition of excess EDTA or 1 M NaCl.

agglutinate liposomes composed of *E. coli* lipids and that agglutination occurs in two distinct fashions. L-CRP exhibits a Ca^{2+}-dependent binding to liposomes (Figure 8), which is inhibited, and indeed reversed (Figure 8, inset), by the presence of excess EDTA or 1.0 M NaCl, and a Ca^{2+}-independent binding that is insensitive to EDTA or ionic strength (Figure 9). The Ca^{2+}-dependent binding is seen as a rapid and large increase in the 90° light-scattering intensity of liposome suspensions. The Ca^{2+}-independent binding is much slower, and since we are essentially measuring the rate of agglutination we employed a higher concentration of L-CRP merely to facilitate the observation of the light-scattering signal. The Ca^{2+}-dependent increase in light-scattering intensity is apparently the result of both agglutination of the vesicles and an increase in the hydrodynamic radius of the liposomes that results from the decoration of the surface with aggregated L-CRP. Electron microscopic examination of

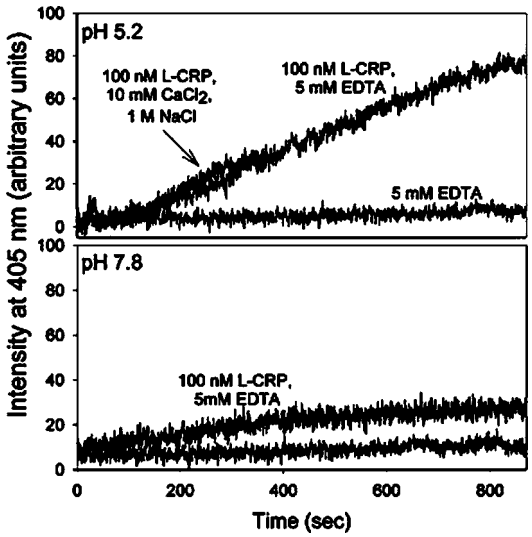

Figure 9 L-CRP agglutinates liposomes in a Ca^{2+}-independent fashion

The 90° light-scattering intensity (405 nm) of a suspension of unilamellar liposomes constructed from total *E. coli* lipids was monitored as an indicator of relative particle size. An increase in 90° light-scattering intensity (405 nm) is observable when 100 nM L-CRP is added to assays containing 5 mM EDTA or to assays containing 10 mM $CaCl_2$, 1 M NaCl (cuvette buffer, pH 5.2). Liposome-binding activity increases at more acidic pH, yet is still observable at pH 7.8.

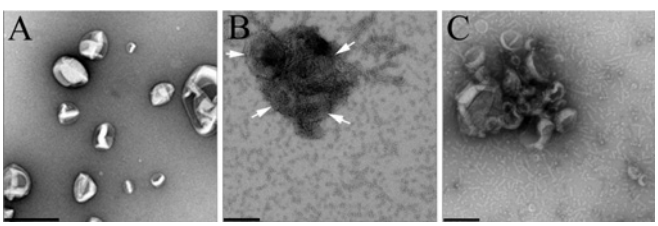

Figure 10 TEM micrographs of L-CRP-bound liposomes

(**A**) Liposomes alone (total *E. coli* lipids). (**B**) L-CRP-bound liposomes in the presence of 10 mM $CaCl_2$. The L-CRP is aggregated into long fibrils that bind to liposomes and extend beyond their borders. Arrows indicate the profiles of liposomes in this Figure. (**C**) L-CRP-bound liposomes in 10 mM EDTA. Short fibrils are present that are not always associated with the surfaces of liposomes. Scale bar = 200 nm.

liposomes treated with L-CRP under these low pH, Ca^{2+}-containing conditions (Figure 10) reveals a large accumulation of hyperoligomerized L-CRP fibres that effectively encapsulate the liposomes (Figure 10B). L-CRP fibres organize into sheet-like structures with oligomerized fibres of protein protruding beyond the boundaries of the agglutinated liposomes. Liposomes treated with L-CRP in cuvette buffer, pH 5.2, 10 mM EDTA (Figure 10C) or cuvette buffer, pH 5.2, 10 mM $CaCl_2$, 1.0 M NaCl (results not shown) appear clumped together. Although short rods of L-CRP are present, these agglutinated liposomes lack the dense coating of hyperoligomerized L-CRP molecules seen at low ionic strength and in the presence of Ca^{2+}.

Consistent with the pore-forming activity, both membrane-binding rates were enhanced at acidic pH. Interestingly, the Ca^{2+}-independent form of binding is observable at pH 7.8. Both forms of binding are observed with liposomes prepared from mixed lipids of natural origin, particularly *E. coli* total lipid extracts. Neither the Ca^{2+}-dependent nor Ca^{2+}-independent binding is seen with liposomes composed of purified egg PC or egg PC/PS (3:1 by mass). Additionally, we did not observe an increase in

light scattering when assaying binding of the LPx to liposomes composed of egg PC and submicellar amounts of lyso-PC or lyso-PE.

DISCUSSION

It has long been known that pentraxins from mammals bind foreign and damaged cell membranes [24,25,37]. These binding activities are reportedly reversed by the addition of EDTA or competitive phosphoamino compounds such as phosphorylethanolamine. Thus they presumably do not entail insertion of the proteins into the hydrophobic regions of the lipid bilayer. Pentraxins from the horseshoe crab do exhibit membrane interaction as revealed by binding and agglutination of bacteria [18,27,28] and the agglutination and haemolysis of mammalian erythrocytes by limulin [16], and we have observed both Ca^{2+}-dependent and Ca^{2+}-independent binding of L-CRP to lipid bilayers. L-CRP and L-SAP lack haemolytic activity. This may be due to an absence of docking sites for these proteins at the red cell surface, a function served by the terminal sialic acids of cell-surface glycoconjugates for limulin. In the present study we have shown that all of the LPx exhibit membrane-permeabilizing activity. Our liposome-based assays revealed such activity against liposomes composed of extracted lipids from both soybean and *E. coli*, and we observed distinct pore formation in asymmetric planar lipid bilayers that mimic the outer membrane of Gram-negative bacteria. In these experiments, L-CRP targets deep rough-type LPS extracted from *E. coli* WBB01. This is consistent with the identification of CrCRP as a major LPS-binding protein [26]. It is certainly a possibility that LPS-binding is also the necessary step in the permeabilization of liposomes composed of *E. coli* lipids.

The presence of PC or PE, the polar headgroups of which are well-known pentraxin ligands, was not sufficient for LPx-mediated permeabilization. It may be the case that lamellar packing of phospholipids sterically inhibits access of the pentraxin phosphocholine/phosphoethanolamine-binding pocket to the targeted areas of the bilayer headgroups. It has been shown that pentraxin bound Ca^{2+} ions directly interact with the phosphate of phosphoamino ligands [6,38]. It is thus likely that adjacent bilayer lipid headgroups provide effective steric hindrance, blocking access to the relatively buried phosphate moiety. This interpretation is strongly supported by studies of mammalian pentraxins that showed that exposure of PC or PE headgroups above the normal bilayer interface, through the incorporation of a linker arm between the glycerol and phosphate moieties, facilitates membrane binding [39,40].

We show that the bilayer of liposomes permeabilized by L-CRP remains intact. The observation of a transient diffusion potential in liposomes pre-incubated with L-CRP over a time period sufficient to induce 100 % dissipation of the valinomycin-induced K^+-diffusion potential under normal assay procedures indicates that the liposomal bilayers retain lamellar structure during their interaction with L-CRP (Figure 5). Target liposomes do not experience fragmentation or a detergent-like solubilization when treated with L-CRP. Additionally, it does not appear that L-CRP exhibits fusogenic activity. This interpretation is supported by the reversibility of the L-CRP-induced increase in the relative particle size of liposomes as seen with light scattering, and the appearance of intact liposomes when viewed with electron microscopy. It is also consistent with the haemolytic activity of limulin. Erythrocyte membranes treated with limulin remain intact as indicated by the reversible ability of extracellular dextrans to inhibit haemoglobin release [23]. These results suggest that the LPx form stable transmembrane pores without inducing large-scale disruption of bilayer structure. Indeed, planar lipid bilayer experiments reveal the formation of distinct pores. The estimated pore diameter from electrical current measurements across the planar lipid bilayer gave a mean value of 1.9 ± 0.2 nm, in good agreement with the estimated functional pore size (1.7 nm) for limulin-mediated haemolysis.

The rapid Ca^{2+}-dependent mode of binding, observed with 90° light scattering, is inhibited in the presence of the Ca^{2+} chelator EDTA or by competition for cationic binding sites with a high concentration of NaCl. The Ca^{2+}-independent mode of binding is not susceptible to either EDTA or high salt. The relatively slow rate of agglutination requires that an increase in protein concentration be utilized to observe the light scattering signal increase. Because pore formation is not sensitive to high ionic strength, we suggest that the slower Ca^{2+}-independent binding observed with light scattering is sufficient for membrane pore formation by L-CRP and that Ca^{2+}-dependent binding is not required. Indeed, at high ionic strength we see a significant increase in the pore-forming activity of L-CRP. Examination of L-CRP-decorated liposomes by electron microscopy shows that the protein oligomers experience higher-order oligomerization in the presence of Ca^{2+} to form long, linearly aggregated protein fibres lying lengthwise on the surfaces of the liposomes. We suggest that the reduced activity at low ionic strength is due to either a sequestration of L-CRP molecules that have bound liposomes in a non-productive Ca^{2+}-dependent manner or to linear aggregation that renders L-CRP incapable of participating in the formation of transmembrane pores, i.e. the pool of L-CRP molecules available to bind in a Ca^{2+}-independent manner is larger at high ionic strength, or both. Calcein leakage assays are routinely performed at stoichiometric values of approx. 250 L-CRP molecules per liposome (results not shown). However, if we assume that L-CRP molecules that have bound in a Ca^{2+}-dependent fashion are effectively inhibited from operating in pore formation, the stoichiometry is not representative of the actual number of pores per vesicle. It may be the case that Ca^{2+} operates in some later step in the permeabilization process, such as induction of a conformational change in membrane-bound L-CRP necessary for protein insertion across the lipid bilayer. Consistent with the suggestion that multiple steps are involved in pore formation, kinetic analysis of L-CRP-induced liposome permeabilization indicated a significant lag phase after the addition of L-CRP followed by a dose-dependent rate of calcein leakage. This lag phase is not apparent when monitoring Ca^{2+}-dependent binding of L-CRP to liposomes.

The insensitivity of L-CRP-generated pore formation to high salt concentrations is similar to the haemolytic activity of limulin, which is optimal at the highest ionic strength tested, 0.29 M NaCl [16]. This is necessary for a protein operating in the plasma of *Limulus*, which has a salt content identical with that of seawater, 0.5 M NaCl [30]. The pH-dependence, however, is not readily explainable. The dependence on low pH suggests that protonation of anionic groups, of protein and/or phospholipid origin, is required for pore formation by L-CRP. The titration of these negatively charged moieties may facilitate contact between protein and target binding sites on the bilayer interface and certainly the overall hydrophobicity of L-CRP increases as the pH is lowered. Membrane-binding and transmembrane insertion by a variety of peptides and proteins, notably the amoebapores [41] and annexins [42] respectively, are modulated by pH. These are examples of mainly intracellular effectors where membrane activity operates in the acidic environment of secondary lysosomes. In the case of the LPx, a localized low pH may occur where the secretory blood cells, the haemocytes, degranulate after encountering LPS [43], analogous to the secretion of protons by activated human neutrophils [44], or when LPx-coated

particles are phagocytosed [45] and permeabilization occurs later in response to the low pH of secondary lysosomes.

Of possible importance for membrane insertion is a predicted N-terminal hydrophobic region present in each of the LPx (results not shown). N-terminal amino acid sequences are largely conserved between limulin and L-CRP and are identical with residue 44. L-SAP differs, sharing only 14 of the first 53 N-terminal residues at conserved positions. The presence of a predicted transmembrane domain in each of the LPx suggests that this region may be important for their biological function and is consistent with the proposal that membrane interaction is part of this function. The human pentraxins, including CRP (NCBI accession # CAA39671), SAP [46] and the newly described neuronal pentraxins [47], all lack a predicted transmembrane region. We are not aware of reports describing membrane permeabilization by human or mammalian pentraxins, a function that in mammals is primarily served by the complement system [48]. If the N-terminal stretch of amino acids is indeed the portion of the protein that inserts across the lipid bilayer, two scenarios of conformational rearrangement for the stable insertion of the LPx suggest themselves: (i) the monomers simply rotate outwards such that the previously buried N-terminus is now exposed at the surface of the pentraxin oligomer, maintaining the original double-stack configuration, or (ii) the individual rings remain intact but separate from each other to expose the hydrophobic N-terminus. The estimated functional pore sizes of 1.9 nm from planar lipid bilayer experiments and 1.7 nm for erythrocyte-associated limulin [23] correspond well with the size of the pore seen in electron micrographs of solution-phase LPx [19], consistent with a model in which the LPx oligomer retains the large central pore during its insertion across the lipid bilayer.

The ability of the *Limulus* pentraxins to permeabilize lipid bilayers suggests that they serve the immune defences of the animal by contributing to the cytolysis of invading pathogens. Indeed, Tan et al. [28] report bactericidal activity from recombinant CrCRP, and we have observed antimicrobial activity against *E. coli* WBB01 (the source strain for LPS utilized in planar bilayer experiments), *E. coli* D31 and *Bacillus megaterium* (see Supplementary Table S1 at http://www.BiochemJ.org/bj/413/bj4130305add.htm). Although cytolytic destruction of foreign cells is an important strategy of immune defence, different phyla of metazoans employ quite different suites of proteins and peptide cytolysins to accomplish this process [20], with the complement system serving as the principal plasma-based agent in mammals [48] and, potentially, the pentraxins as the principle effectors in the plasma of *Limulus* [16]. The mechanism of bacterial targeting by horseshoe crab pentraxins is not fully understood. Our planar bilayer experiments and previous reports strongly suggest that binding of LPS is the primary step in the recognition of Gram-negative bacteria [28]. Interactions with plasma components modify the bacterial binding behaviour of CrCRP; galactose-binding protein and carcinolectin-5 participate in a protein complex with CrCRP to recognize diverse bacterial targets under conditions where divalent cations are not present [27]. It may be the case that this complex acts in an analogous fashion to the complement system, where plasma components recruit cytolytic effector molecules, in this case pentraxin proteins, to the surface of the target pathogen. The blood cells of *Limulus* contain cytolytic peptides that presumably reinforce the cytolytic activities of the LPx once blood cell exocytosis has released these agents into the serum [49,50]. Future studies should be directed at understanding the fate of pentraxin-bound microbes, i.e. phagocytosis, cytolysis, and what role the interactions of other plasma proteins with the pentraxins play in determining that fate.

We thank Claudia Ott for technical help in the early phase of this study, Dr Friederich Buck (Institute of Biochemistry and Molecular Biology, University of Hamburg, Hamburg, Germany) for protein sequencing, Dr Irwin Segel (Department of Biology, University of California, Davis, CA, U.S.A.) for indispensable discussion concerning the kinetic analysis and Dr John Crowe (College of Biological Sciences, University of California, Davis, CA, U.S.A.) for critical reading of the manuscript. This research was supported by Grant 0344360 from the National Science Foundation (to P.B.A.), Bavaria California Technology Center grant (to J.M.H., M.L. and P.B.A.), grant SFB 617 from the German Research Council (to M.L. and T.G.) and by the National Institutes of Health grant U54 GM074929 (to H.T.C. and H.S.).

REFERENCES

1 Gewurz, H., Zhang, X.-H. and Lint, T. F. (1995) Structure and function of the pentraxins. Curr. Opin. Immunol. **7**, 54–64
2 Macleod, C. M. and Avery, O. (1941) The occurrence during acute infection of a protein not normally present in the blood (II). J. Exp. Med. **73**, 183–190
3 Garlanda, C., Bottazzi, B., Bastone, A. and Mantovani, A. (2005) Pentraxins at the crossroads between innate immunity, inflammation, matrix deposition, and female fertility. Annu. Rev. Immunol. **23**, 337–366
4 Pepys, M. B. and Hirschfield, G. M. (2003) C-reactive protein: a critical update. J. Clin. Invest. **111**, 1805–1812
5 Labarrere, C. A. and Zaloga, G. P. (2004) C-reactive protein: from innocent bystander to pivotal mediator of atherosclerosis. Am. J. Med. **117**, 499–507
6 Emsley, J., White, H. E., O'Hara, B. P., Oliva, G., Srinivasan, N., Tickle, I. J., Blundell, T. L., Pepys, M. B. and Wood, S. P. (1994) Structure of pentameric human serum amyloid P component. Nature **367**, 338–345
7 Garlanda, C., Hirsch, E., Bozza, S., Salustri, A., De Acetis, M., Nota, R., Maccagno, A., Riva, F., Bottazzi, B., Peri, G. et al. (2002) Non-redundant role of the long pentraxin PTX3 in anti-fungal innate immune response. Nature **420**, 182–186
8 Mantovani, A., Garlanda, C., Doni, A. and Bottazzi, B. (2008) Pentraxins in innate immunity: from C-reactive protein to the long pentraxin PTX3. J. Clin. Immunol. **28**, 1–13
9 Robey, F. A. and Liu, T. Y. (1981) Limulin: a C-reactive protein from *Limulus polyphemus*. J. Biol. Chem. **256**, 969–975
10 Nguyen, N. Y., Suzuki, A., Cheng, S. M., Zon, G. and Liu, T. Y. (1986) Isolation and characterization of *Limulus* C-reactive protein genes. J. Biol. Chem. **261**, 10450–10455
11 Nguyen, N. Y., Suzuki, A., Boykins, R. A. and Liu, T. Y. (1986) The amino acid sequence of *Limulus* C-reactive protein. Evidence of polymorphism. J. Biol. Chem. **261**, 10456–10465
12 Shrive, A. K., Metcalfe, A. M., Cartwright, J. R. and Greenhough, T. J. (1999) C-reactive protein and SAP-like pentraxin are both present in *Limulus polyphemus* haemolymph: crystal structure of Limulus SAP. J. Mol. Biol. **290**, 997–1008
13 Tharia, H. A., Shrive, A. K., Mills, J. D., Arme, C., Williams, G. T. and Greenhough, T. J. (2002) Complete cDNA sequence of SAP-like pentraxin from *Limulus polyphemus*: implications for pentraxin evolution. J. Mol. Biol. **316**, 583–597
14 Roche, A. C. and Monsigny, M. (1974) Purification and properties of limulin: a lectin (agglutinin) from hemolymph of *Limulus polyphemus*. Biochim. Biophys. Acta **371**, 242–254
15 Kaplan, R., Li, S. S. and Kehoe, J. M. (1977) Molecular characterization of limulin, a sialic acid binding lectin from the hemolymph of the horseshoe crab, *Limulus polyphemus*. Biochemistry **16**, 4297–4303
16 Armstrong, P. B., Swarnakar, S., Srimal, S., Misquith, S., Hahn, E. A., Aimes, R. T. and Quigley, J. P. (1996) A cytolytic function for a sialic acid-binding lectin that is a member of the pentraxin family of proteins. J. Biol. Chem. **271**, 14717–14721
17 Armstrong, P. B., Armstrong, M. T. and Quigley, J. P. (1993) Involvement of α_2-macroglobulin and C-reactive protein in a complement-like hemolytic system in the arthropod, *Limulus polyphemus*. Mol. Immunol. **30**, 929–934
18 Iwaki, D., Osaki, T., Mizunoe, Y., Wai, S. N., Iwanaga, S. and Kawabata, S. (1999) Functional and structural diversities of C-reactive proteins present in horseshoe crab hemolymph plasma. Eur. J. Biochem. **264**, 314–326
19 Fernandez-Moran, H., Marchalonis, J. J. and Edelman, G. M. (1968) Electron microscopy of a hemagglutinin from *Limulus polyphemus*. J. Mol. Biol. **32**, 467–469
20 Yeaman, M. R. and Yount, N. Y. (2003) Mechanisms of antimicrobial peptide action and resistance. Pharmacol. Rev. **55**, 27–55
21 Müller-Eberhard, H. J. (1986) The membrane attack complex of complement. Annu. Rev. Immunol. **4**, 503–528
22 Müller-Eberhard, H. J. (1988) Molecular organization and function of the complement system. Annu. Rev. Biochem. **57**, 321–347
23 Swarnakar, S., Asokan, R., Quigley, J. P. and Armstrong, P. B. (2000) Binding of α_2-macroglobulin and limulin: regulation of the plasma haemolytic system of the American horseshoe crab, *Limulus*. Biochem. J. **347**, 679–685

24 Volanakis, J. E. and Wirtz, K. W. (1979) Interaction of C-reactive protein with artificial phosphatidylcholine bilayers. Nature **281**, 155–157
25 Chang, M. K., Binder, C. J., Torzewski, M. and Witztum, J. L. (2002) C-reactive protein binds to both oxidized LDL and apoptotic cells through recognition of a common ligand: phosphorylcholine of oxidized phospholipids. Proc. Natl. Acad. Sci. U.S.A. **99**, 13043–13048
26 Ng, P. M. L., Jin, Z., Tan, S. S. H., Ho, B. and Ding, J. L. (2004) C-reactive protein: a predominant LPS-binding acute phase protein responsive to *Pseudomonas* infection. J. Endotoxin Res. **10**, 163–174
27 Ng, P. M., Le Saux, A., Lee, C. M., Tan, N. S., Lu, J., Thiel, S., Ho, B. and Ding, J. L. (2007) C-reactive protein collaborates with plasma lectins to boost immune response against bacteria. EMBO J. **26**, 3431–3440
28 Tan, S. S. H., Ng, P. M. L., Ho, B. and Ding, J. L. (2005) The antimicrobial properties of C reactive protein (CRP). J. Endotoxin Res. **11**, 249–256
29 Galanos, C., Luderitz, O. and Westphal, O. (1969) A new method for the extraction of R lipopolysaccharides. Eur. J. Biochem. **9**, 245–249
30 Armstrong, P. B., Rossner, M. T. and Quigley, J. P. (1985) An α_2-macroglobulinlike activity in the blood of chelicerate and mandibulate arthropods. J. Exp. Zool. **236**, 1–9
31 Loew, L. M., Rosenberg, I., Bridge, M. and Gitler, C. (1983) Diffusion potential cascade. Convenient detection of transferable membrane pores. Biochemistry **22**, 837–844
32 Pick, U. (1981) Liposomes with a large trapping capacity prepared by freezing and thawing of sonicated phospholipid mixtures. Arch. Biochem. Biophys. **212**, 186–194
33 Montal, M. and Mueller, P. (1972) Formation of bimolecular membranes from lipid monolayers and a study of their electrical properties. Proc. Natl. Acad. Sci. U.S.A. **69**, 3561–3566
34 Wiese, A. and Seydel, U. (2000) Electrophysiological measurements on reconstituted outer membranes. Methods Mol. Biol. **145**, 355–370
35 Osborn, M. J., Gander, J. E., Parisi, E. and Carson, J. (1972) Mechanism of assembly of the outer membrane of *Salmonella typhimurium*. Isolation and characterization of cytoplasmic and outer membrane. J. Biol. Chem. **247**, 3962–3972
36 Shaw, N. (1974) Lipid composition as a guide to the classification of bacteria. Adv. Appl. Microbiol. **17**, 63–108
37 Gershov, D., Kim, S., Brot, N. and Elkon, K. B. (2000) C-reactive protein binds to apoptotic cells, protects the cells from assembly of the terminal complement components, and sustains an antiinflammatory innate immune response: implications for systemic autoimmunity. J. Exp. Med. **192**, 1353–1364
38 Shrive, A. K., Cheetham, G. M., Holden, D., Myles, D. A., Turnell, W. G., Volanakis, J. E., Pepys, M. B., Bloomer, A. C. and Greenhough, T. J. (1996) Three dimensional structure of human C-reactive protein. Nat. Struct. Biol. **3**, 346–354
39 Sui, S. F., Sun, Y. T. and Mi, L. Z. (1999) Calcium-dependent binding of rabbit C-reactive protein to supported lipid monolayers containing exposed phosphorylcholine group. Biophys. J. **76**, 333–341
40 Wang, H. W. and Sui, S. (1999) Pentameric two-dimensional crystallization of rabbit C-reactive protein on lipid monolayers. J. Struct. Biol. **127**, 283–286
41 Andrä, J., Herbst, R. and Leippe, M. (2003) Amoebapores, archaic effector peptides of protozoan origin, are discharged into phagosomes and kill bacteria by permeabilizing their membranes. Dev. Comp. Immunol. **27**, 291–304
42 Hegde, B. G., Isas, J. M., Zampighi, G., Haigler, H. T. and Langen, R. (2006) A novel calcium independent peripheral membrane-bound form of annexin B12. Biochemistry **45**, 934–942
43 Armstrong, P. B. and Rickles, F. R. (1982) Endotoxin-induced degranulation of the *Limulus* amebocyte. Exp. Cell Res. **140**, 15–24
44 van Zwieten, R., Wever, R., Hamers, M. N., Weening, R. S. and Roos, D. (1981) Extracellular proton release by stimulated neutrophils. J. Clin. Invest. **68**, 310–313
45 Armstrong, P. B. and Levin, J. (1979) *In vitro* phagocytosis by *Limulus* blood cells. J. Invertebr. Pathol. **34**, 145–151
46 Ohnishi, S., Maeda, S., Shimada, K. and Arao, T. (1986) Isolation and characterization of the complete complementary and genomic DNA sequences of human serum amyloid P Component. J. Biochem. **100**, 849–858
47 Strausberg, R. L., Feingold, E. A., Grouse, L. H., Derge, J. G., Klausner, R. D., Collins, F. S., Wagner, L., Shenmen, C. M., Schuler, G. D., Altschul, S. F. et al. (2002) Generation and initial analysis of more than 15000 full length human and mouse cDNA sequences. Proc. Natl. Acad. Sci. U.S.A. **99**, 16899–16903
48 Law, S. K. A. and Reid, K. B. M. (1995) Complement, Oxford University Press, New York
49 Nakamura, T., Furunaka, H., Miyata, T., Tokunaga, F., Muta, T., Iwanaga, S., Niwa, M., Takao, T. and Shimonishi, Y. (1988) Tachyplesin, a class of antimicrobial peptide from the hemocytes of the horseshoe crab (*Tachypleus tridentatus*). Isolation and chemical structure. J. Biol. Chem. **263**, 16709–16713
50 Park, N. G., Lee, S., Oishi, O., Aoyagi, H., Iwanaga, S., Yamashita, S. and Ohno, M. (1992) Conformation of tachyplesin I from *Tachypleus tridentatus* when interacting with lipid matrices. Biochemistry **31**, 12241–12247

Received 2 October 2007/14 March 2008; accepted 28 March 2008
Published as BJ Immediate Publication 28 March 2008, doi:10.1042/BJ20071357